

switch (see **D**). For given serum stimulation strength and parameter set, the R-point is reversely correlated to the basal maintenance serum level. (**D**) Simulated serum responses of E2F steady-state affected by parameter changes. All parameter changes in **C** resulted in the same E2F switching threshold ($Th = 1.6$, up-pointing black arrow) but different E2F *deactivation* thresholds (shown between the green and red down-pointing arrows in 3 color groups according to the threshold values). For a given parameter set, 1) the activation and deactivation thresholds refer to the lowest serum concentration resulting in the E2F-ON steady state in simulations with the E2F-OFF and -ON initial conditions, respectively; and 2) the serum range between the activation and deactivation thresholds defines the bistable region of the Rb-E2F switch. (**E**) Tipping point of Rb/E2F abundance affected by parameter changes. The amounts of unphosphorylated Rb and free form of E2F were examined in time course simulations: initially, Rb abundance was in excess over E2F ($Rb/E2F > 1$); over time with serum input, the amount of Rb decreased and that of E2F increased; up to a time point (the tipping point), $Rb/E2F = 1$, and from then on $Rb/E2F < 1$. The simulated tipping point (y-axis) corresponding to increasing parameter values of kI and kR is shown (serum input = 10%).

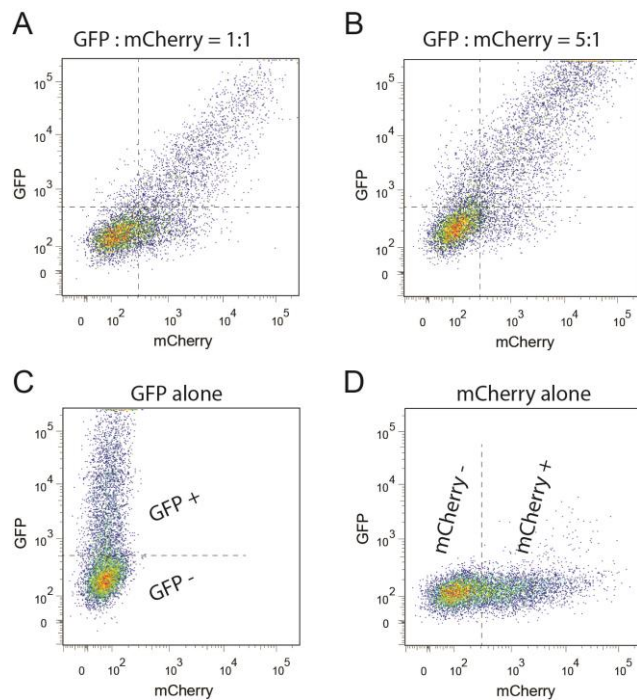


Figure S2. Linear correlation between levels of co-transfected expression vectors. Related to Figure 5.

GFP and mCherry expression vectors were co-transfected into REF52 cells using a Neon electroporator. Given a mixing ratio of GFP:mCherry = 1:1, a small but noticeable subset of mCherry+ cells did not exhibit the GFP+ signal (**A**). With a mixing ratio of GFP:mCherry = 5:1, nearly all mCherry+ cells exhibited the GFP+ signal and the GFP fluorescence intensity was linearly correlated with the mCherry fluorescence intensity in individual cells (**B**). Since both GFP and mCherry are stable proteins with similar long half-lives (Corish and Tyler-Smith, 1999; Shaner et al., 2004), the linear correlation between GFP and mCherry signals indicated a linear correlation between the numbers of introduced GFP and mCherry vectors via co-transfection. The ratio of 5:1 was then used in this study for the co-transfection of protein expression vectors and the mCherry vector. Shown in (**C**) and (**D**) are the GFP-only and mCherry-only transfection controls, respectively.

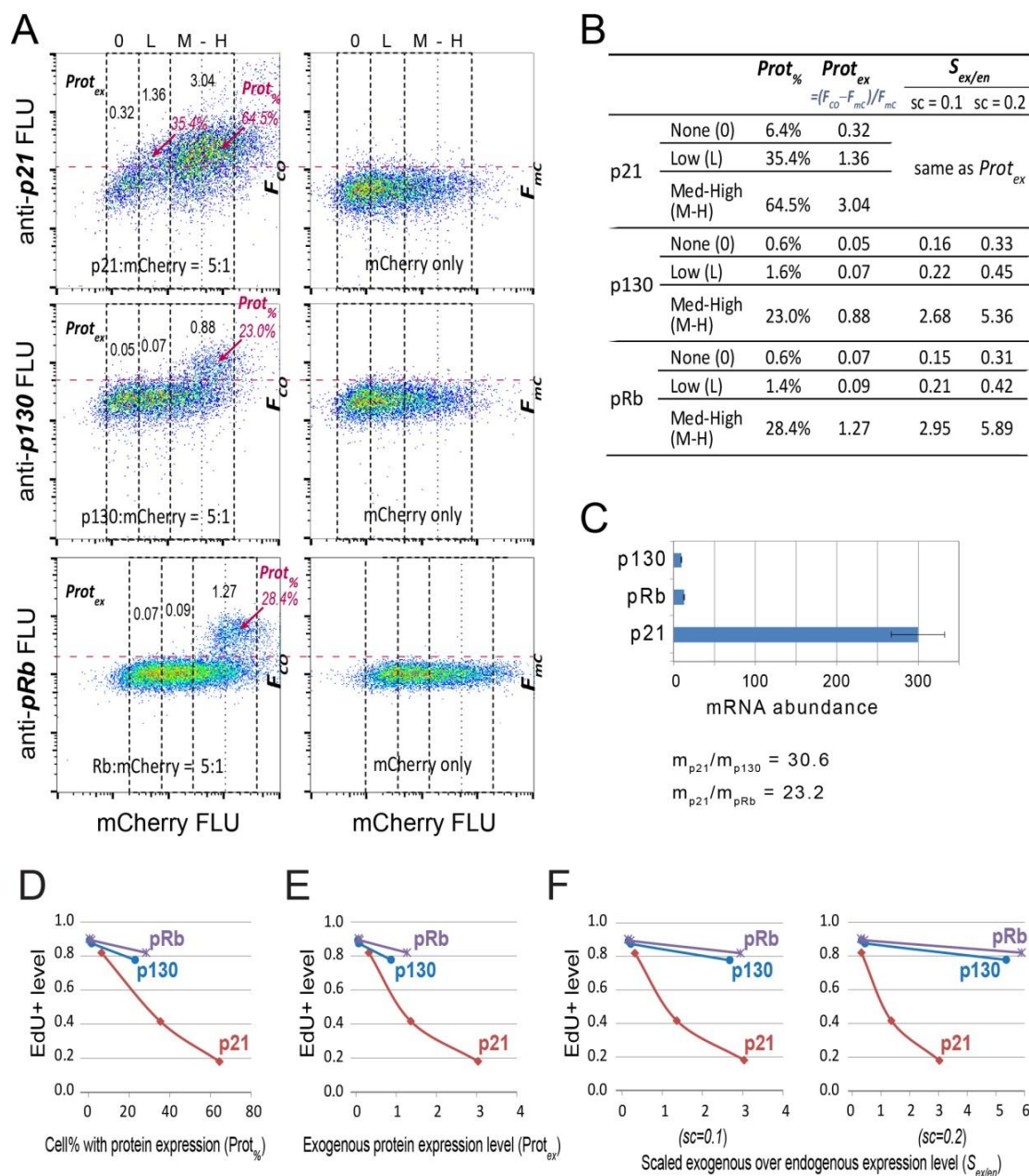


Figure S3. Correlate p21, p130, and pRb expression vector levels with protein levels. Related to Figure 5.

(A,B) Measure the correlation between levels of protein expression and introduced expression vector. Expression vectors of p21, p130, and pRb were co-transfected with the mCherry vector (5:1 ratio) as in Figure 5A. Cells were induced to quiescence by serum starvation and then subject to immunoflow cytometry with protein-specific antibodies (see Methods). Y-axis = antibody-specific fluorescence intensity (FLU). X-axis = mCherry intensity. 0, L, M, H = cell bins of non-transfected, and with low, medium, and high levels of the mCherry vector, respectively, as in Figure 5A. $Prot_{\%}$ corresponds to the percentage of cells in each bin with positive ectopic protein expression (with antibody-specific FLU over the mCherry-only control). $Prot_{ex} = (F_{CO} - F_{mC}) / F_{mC}$ represents the FLU fold-increase over background due to introduced expression vector, with F_{CO} and F_{mC} being the mean antibody-fluorescence intensities in the samples of co-transfection and mCherry-only transfection control, respectively. F_{mC} represents the combination of endogenous protein staining and non-specific background staining (the major source of F_{mC} , as seen from the similarly high fluorescence intensity with anti-FLAG antibody (no endogenous staining) in Figure S5). (B) Estimate protein level increase due to exogenous expression. $S_{ex/en} = Prot_{ex} / L_{en}$ (L_{en} , relative endogenous protein level)

represents the scaled exogenous protein level normalized by endogenous expression. The fold difference of two endogenous protein levels was converted from the fold difference of their mRNA abundance (measured in **C**) by a given scaling factor ($sc = 0.1$ or 0.2 ; e.g., when L_{en} of p21 was set to 1, L_{en} of pRb = $1/(sc * m_{p21}/m_{pRb})$). **(C)** mRNA abundance. The transcript abundance (x-axis) of endogenous p21, pRb, and p130 was quantified from RNA-seq analysis of 2D-STA cells and consistent with qRT-PCR results (Fujimaki, Bai, and Yao, unpublished). The fold differences of mRNA abundance are shown at the bottom. **(D-F)** Convert expression vector levels to relative exogenous protein levels. The conversion was based on **B**, using $Prot_{\%}$ (**D**, same as Figure 5C), $Prot_{ex}$ (**E**), and $S_{ex/en}$ with $sc=0.1$ (**F**, left; same as Figure 5D) and $sc=0.2$ (**F**, right), respectively. X-axis = correspondingly converted units (left to right data points: 0, L, M-H). Y-axis = EdU+ cell proportion as determined in Figure 5B. Different assumed sc values did not affect the qualitative feature of the results, as seen in **F**.

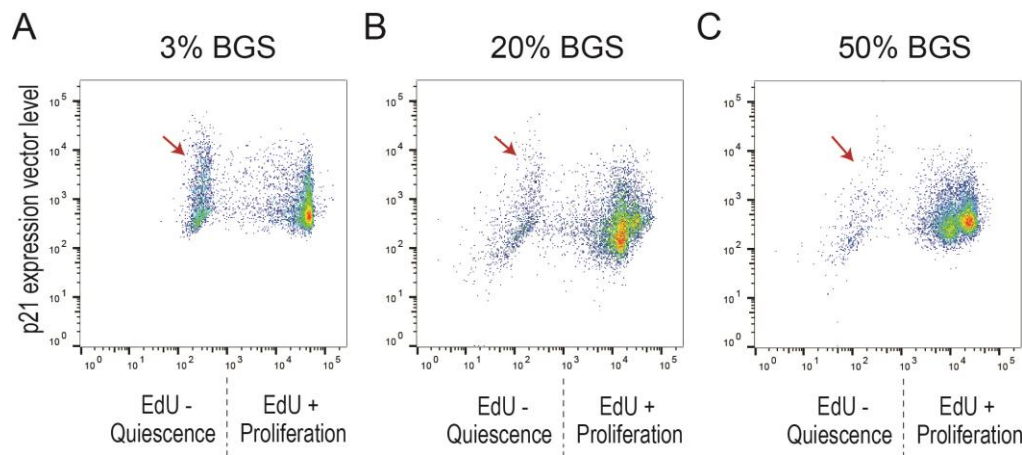


Figure S4. High ectopic p21 expression leads to deep quiescence but not senescence. Related to Figure 5. Quiescent cells (2D-STA) with transfected p21 were switched to medium containing serum at indicated concentrations and EdU at time 0. Cells were harvested 48 hours later for EdU incorporation assay. Y-axis = levels of introduced p21 expression vector in individual cells (as in Figure 5A). X-axis = EdU-incorporation intensity. Red arrow indicates non-proliferative (EdU-) cells with high p21 expression; this subpopulation of cells diminished with serum stimulation at high concentrations (20% and 50% vs. 3%), indicating that those cells were not senescent but in deep quiescence.

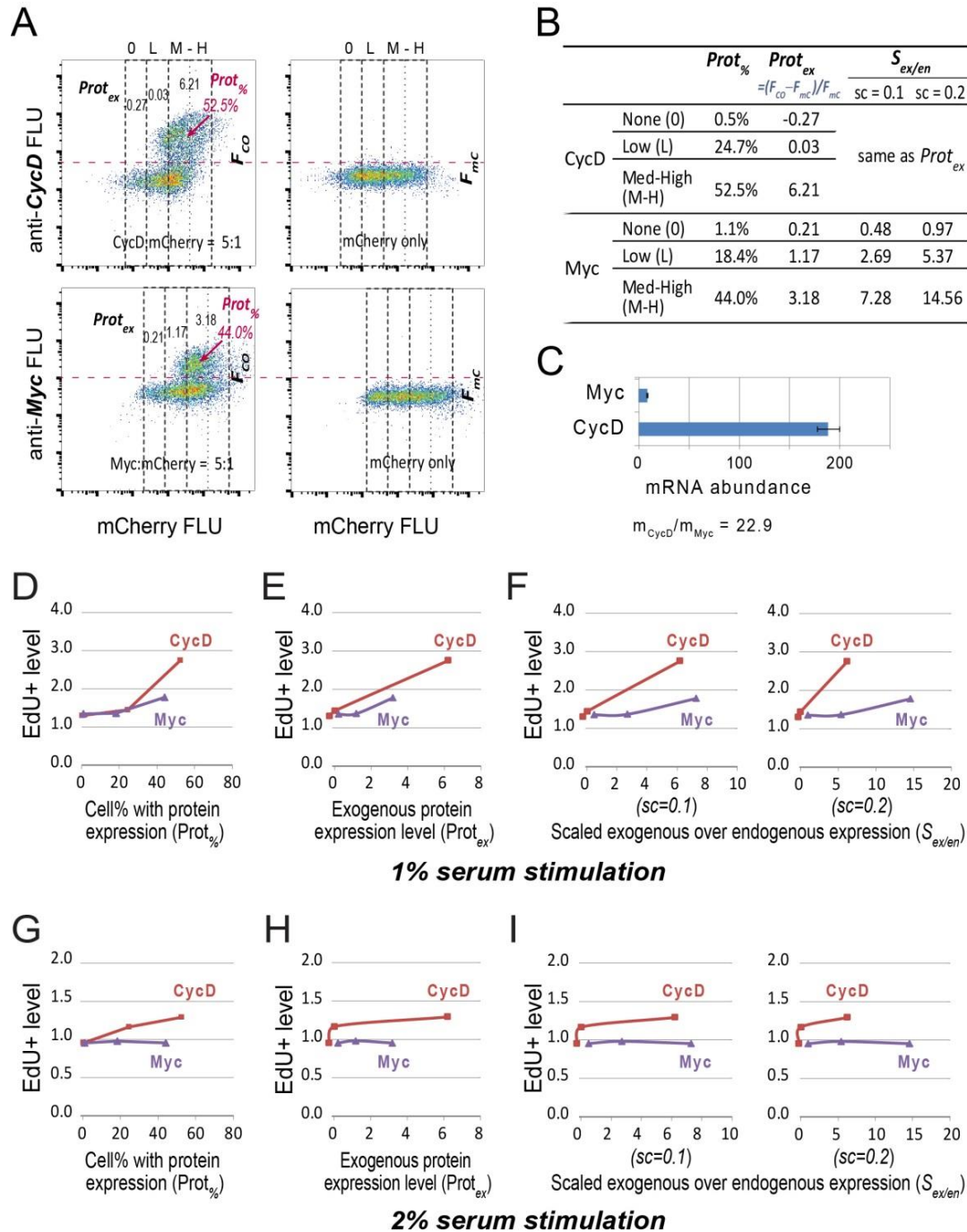


Figure S5. Correlate CycD and Myc expression vector levels with protein levels. Related to Figure 6.
(A,B) Measure the correlation between levels of protein expression and introduced expression vector. Expression vectors of CycD and Myc were co-transfected with the mCherry vector (5:1 ratio) as in Figure 6A. Cells were induced to quiescence by serum starvation and then subject to immunoflow cytometry with protein-specific antibodies (see Methods). Y-axis = antibody-specific fluorescence intensity (FLU). X-axis = mCherry intensity. 0, L, M, H = non-transfected, with low, medium, and high levels of the mCherry vector, respectively, as in Figure 6A. $Prot_{\%}$, $Prot_{ex}$, F_{CO} , and F_{MC} are as defined in Figure S3A. **(B)** Estimate protein level increase due to exogenous expression. The scaled exogenous over endogenous expression $S_{ex/en}$ and scaling factor sc are as defined in Figure S3B. **(C)** mRNA abundance. The transcript abundance (x-axis) of endogenous Myc and CycD1 was quantified from RNA-seq analysis of 2D-STA cells and consistent with qRT-PCR results (Fujimaki, Bai, and Yao, unpublished).

The fold difference in the mRNA abundance of CycD1 and Myc (shown at the bottom) was converted to the fold difference in their protein abundance (as in Figure S3B) by a given degree ($sc = 0.1$ or 0.2 in **B**). Different assumed sc values did not affect the qualitative feature of the results (as seen in **F** and **I**). (**D-I**) Convert expression vector levels to relative exogenous protein levels. The conversion was based on **B**, using $Prot\%$ (**D,G**), $Prot_{ex}$ (**E,H**), and $S_{ex/en}$ with $sc=0.1$ (**F,I**, left; same as Figure 6C) and $sc=0.2$ (**F,I**, right), respectively. X-axis = correspondingly converted units (left to right data points: 0, L, M-H). Y-axis = EdU+ cell proportion as determined in Figure 6B.

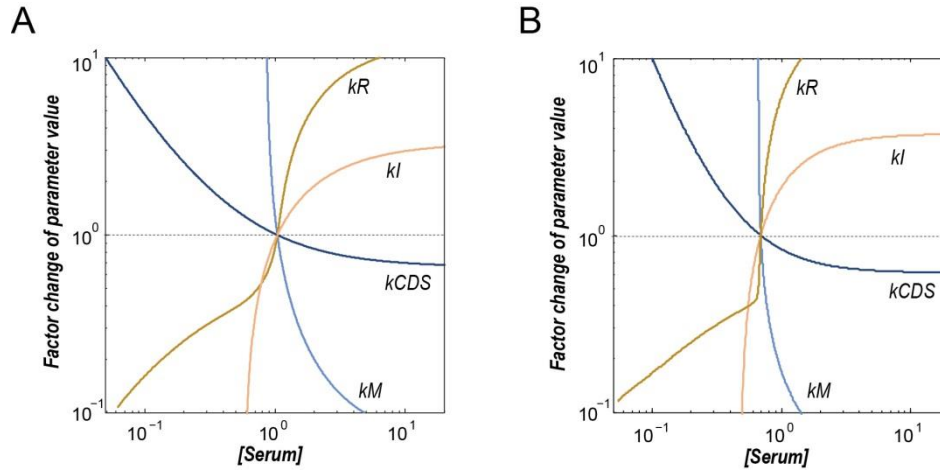


Figure S6. Two-parameter bifurcation diagram. Related to Model Simulations in Experimental Procedures. (**A**) The curves trace out the locations of the saddle-node bifurcation point (in terms of the serum concentration $[S]$ at which the system switches from E2F-OFF to E2F-ON, x-axis) of the Rb-E2F bistable model (Table S1), as a function of a given value of the four experimentally tested parameters kl , kR , $kCDS$, and kM , respectively. Y-axis = factor change of a parameter from its base value (Table S2). (**B**) Same as **A**, except that cooperativity (Hill coefficient = 1.5) was introduced in each Hill function term of the model in **A** and that a small basal synthesis rate $k_{E0} = 0.02$ nM/hr was added to the E2F synthesis term so that the simulated E2F activation dynamics (after all Hill coefficients were increased from 1 to 1.5) was similar to that in the model in **A**.

Table S1. The Rb-E2F switch model. Related to Model Simulations in Experimental Procedures (adapted from (Yao et al., 2008), with additions marked with **).

$\frac{d[M]}{dt} = \frac{k_M[S]}{K_S + [S]} - d_M[M]$
$\frac{d[E]}{dt} = k_E \left(\frac{[M]}{K_M + [M]} \right) \left(\frac{[E]}{K_E + [E]} \right) + \frac{k_b[M]}{K_M + [M]} + \frac{k'_P[CD][RE]}{K_{CD} + [RE]} + \frac{k'_P[CE][RE]}{K_{CE} + [RE]} - d_E[E] - k_{RE}[R][E]$
$\frac{d[CD]}{dt} = \frac{k_{CD}[M]}{K_M + [M]} + \frac{k_{CDS}[S]}{K_S + [S]} - d_{CD}[CD]$
$\frac{d[CE]}{dt} = \frac{k_{CE}[E]}{K_E + [E]} - d_{CE}[CE]$
$\frac{d[R]}{dt} = k_R + \frac{k_{DP}[RP]}{K_{RP} + [RP]} - k_{RE}[R][E] - \frac{k'_P[CD][R]}{K_{CD} + [R]} - \frac{k'_P[CE][R]}{K_{CE} + [R]} - d_R[R]$
$\frac{d[RP]}{dt} = \frac{k'_P[CD][R]}{K_{CD} + [R]} + \frac{k'_P[CE][R]}{K_{CE} + [R]} + \frac{k'_P[CD][RE]}{K_{CD} + [RE]} + \frac{k'_P[CE][RE]}{K_{CE} + [RE]} - \frac{k_{DP}[RP]}{K_{RP} + [RP]} - d_{RP}[RP]$
$\frac{d[RE]}{dt} = k_{RE}[R][E] - \frac{k'_P[CD][RE]}{K_{CD} + [RE]} - \frac{k'_P[CE][RE]}{K_{CE} + [RE]} - d_{RE}[RE]$
$** \frac{d[I]}{dt} = k_I - d_I[I]$
$** \left(k'_P = \frac{k_P}{K_p + [I]} \right)$

Model variables:

S: serum concentration

M: Myc

E: E2F

CD: Cyclin D/Cdk4,6

CE: Cyclin E/Cdk2

R: Rb family proteins

RP: Phosphorylated Rb

RE: Rb-E2F complex

I: Cdk inhibitors

Initial conditions:

[M] = [E] = [CD] = [CE] = [R] = [RP] = 0 nM; [RE] = 0.55 nM; ** [I] = 0.5 nM.

Model parameters:

[See Table S2]

Table S2. Model parameters. Related to Model Simulations in Experimental Procedures (adapted from (Yao et al., 2008), with additions marked with **).

Symbol	Values	Description
k_M	1.0 nM/hr	Rate constant of Myc synthesis driven by growth factors
k_E	0.4 nM/hr	Rate constant of E2F synthesis driven by Myc and E2F
k_b	0.003 nM/hr	Rate constant of E2F synthesis driven by Myc alone
k_{CD}	0.03 nM/hr	Rate constant of CycD synthesis driven by Myc
k_{CDS}	0.45 nM/hr	Rate constant of CycD synthesis driven by growth factors
k_{CE}	0.35 nM/hr	Rate constant of CycE synthesis driven by E2F
k_R	0.18 nM/hr	Rate constant of Rb constitutive synthesis
k_I^{**}	0.15 nM/hr	Rate constant of Cdk inhibitor synthesis
k_{DP}	3.6 nM/hr	Dephosphorylation rate constant of Rb by phosphatases
k_{RE}	180 nM/hr	Association rate constant of Rb and E2F
K_S	0.5 nM	Michaelis-Menten parameter for CycD and Myc synthesis by growth factors
K_E	0.15 nM	Michaelis-Menten parameter for CycE and E2F synthesis by E2F
K_M	0.15 nM	Michaelis-Menten parameter for CycD and E2F synthesis by Myc
K_{RP}	0.01 nM	Michaelis-Menten parameter for Rb dephosphorylation
K_{CD}	0.92 nM	Michaelis-Menten parameter for Rb phosphorylation by CycD/Cdk4,6
K_{CE}	0.92 nM	Michaelis-Menten parameter for Rb phosphorylation by CycE/Cdk2
d_M	0.7/hr	Degradation rate constant of Myc
d_E	0.25/hr	Degradation rate constant of E2F
d_{CD}	1.5/hr	Degradation rate constant of CycD
d_{CE}^*	1.5/hr	Degradation rate constant of CycE
d_R	0.06/hr	Degradation rate constant of Rb
d_{RP}	0.06/hr	Degradation rate constant of phosphorylated Rb
d_{RE}	0.03/hr	Degradation rate constant of Rb-E2F complex
d_I^{**}	0.3/hr	Degradation rate constant of Cdk inhibitor p21 (Schönthal, 2004)
k_P^{**}	45/hr	Phosphorylation rate constant of CycD/Cdk4,6 and CycE/Cdk2 (Cdks)
K_P^{**}	2 nM	Michaelis-Menten parameter for Cdk activities affected by Cdk inhibitors
k'_P	$k_p/(K_p + [I])$	Effective phosphorylation rate constant of CycD/Cdk4,6 and CycE/Cdk2

** The values of the four new parameters were adjusted together so that $k'_p = 18/\text{hr}$ as in (Yao et al., 2008) (with the initial condition $[I] = 0.5 \text{ nM}$) and that the simulated E2F activation dynamics is the same as that in (Yao et al., 2008) for a given serum input.

* $d_{CE} = 3/\text{hr}$ in constructing a quasi-potential landscape from the SDE version of the Rb-E2F switch model (see Methods), to facilitate the system converging at a steady-state distribution of E2F molecule number.

Table S3. Minimum serum duration* required to turn ON the Rb-E2F switch. Related to Figure 4A.

Activation threshold (Th)	Parameter changed	Factor change of parameter	Model time (Hr)	Minimum serum pulse (Hr)	
				40% E2F-ON	50% E2F-ON
0.8	Base (no change)	1.0 (no change)	24	3.0	3.1
			48	3.0	3.1
			108	3.0	3.1
1.6	<i>dI</i>	0.43	24	8.2	10.3
			48	8.2	9.2
			108	8.2	9.2
	<i>kCDS</i>	0.79	24	7.2	7.5
			48	7.2	7.5
			108	7.2	7.5
	<i>kP</i>	0.82	24	12.0	13.3
			48	11.5	12.1
			108	11.5	12.1
	<i>dCD</i>	1.25	24	6.9	7.0
			48	6.9	7.0
			108	6.9	7.0
	<i>KP</i>	1.28	24	12.0	13.9
			48	11.1	12.1
			108	11.1	12.1
	<i>KCD</i>	1.45	24	7.1	8.0
			48	7.1	8.0
			108	7.1	8.0
	<i>KE</i>	1.89	24	20.0	20.3
			48	15.9	16.9
			108	15.9	16.9
	<i>kI</i>	2.04	24	10.0	12.5
			48	9.9	11.0
			108	9.9	11.0
	<i>kRE</i>	2.15	24	7.1	7.7
			48	7.1	7.7
			108	7.1	7.7
	<i>dRE</i>	2.18	24	4.9	5.0
			48	4.9	5.0
			108	4.9	5.0
	<i>KS</i>	2.77	24	7.0	7.9
			48	7.0	7.9
			108	7.0	7.9
	<i>kR</i>	5.53	24	20.3	21.1
			48	16.1	17.1
			108	16.1	17.1

*Serum pulse was applied as in Figure 4A. The minimum serum-pulse duration required to turn ON the Rb-E2F switch in a given percentage (40% or 50%) of cells at the indicated model hours was calculated for each parameter change from 500 stochastic simulations of the Rb-E2F bistable model (Table S1).

Table S4. Source data related to Figure 5B.

#	mC	EdU- (c.c.)	EdU+ (c.c.)	EdU+%	#	p21	EdU- (c.c.)	EdU+ (c.c.)	EdU+%	(c.c., cell count)
1	0	1045	5250	83.4	1	0	1144	2874	71.5	
	L	754	3333	81.6		L	2033	1148	36.1	
	M+H	554	1502	73.1		M+H	1777	382	17.7	
2	0	757	5365	87.6	2	0	1757	3839	68.6	
	L	628	3386	84.4		L	2597	1547	37.3	
	M+H	459	1377	75.0		M+H	2082	423	16.9	
3	0	781	6100	88.6	3	0	1225	2839	69.9	
	L	668	3600	84.3		L	1979	1230	38.3	
	M+H	453	1479	76.6		M+H	1819	409	18.4	
4	0	2293	4398	65.7	4	0	2439	2787	53.3	
	L	1372	2789	67.0		L	3313	1291	28.0	
	M+H	883	1683	65.6		M+H	3734	313	7.7	
5	0	1967	5124	72.3	5	0	1477	2219	60.0	
	L	1110	2676	70.7		L	2835	1012	26.3	
	M+H	1063	2131	66.7		M+H	5125	432	7.8	
6	0	1928	5444	73.8	6	0	1676	2827	62.8	
	L	914	2719	74.8		L	3868	1387	26.4	
	M+H	1018	2345	69.7		M+H	7222	665	8.4	
		<i>s.e.m. (%)</i>	<i>normalized(%)</i>	avg (EdU+%)			<i>s.e.m. (%)</i>	<i>normalized(%)</i>	avg (EdU+%)	
	0	6.8	100.0	78.6		0	5.4	81.9	64.4	
	L	5.5	100.0	77.1		L	3.4	41.6	32.1	
	M+H	3.6	100.0	71.1		M+H	3.1	18.0	12.8	
#	Rb	EdU- (c.c.)	EdU+ (c.c.)	EdU+%	#	p130	EdU- (c.c.)	EdU+ (c.c.)	EdU+%	
1	0	2018	5306	72.4	1	0	2243	4738	67.9	
	L	1434	3025	67.8		L	1647	3046	64.9	
	M+H	981	1134	53.6		M+H	1147	1193	51.0	
2	0	1816	5735	76.0	2	0	1898	4532	70.5	
	L	1280	3157	71.2		L	1286	2494	66.0	
	M+H	797	1116	58.3		M+H	906	886	49.4	
3	0	2065	5463	72.6	3	0	2114	5206	71.1	
	L	1477	3101	67.7		L	1405	3032	68.3	
	M+H	1010	1220	54.7		M+H	1181	1245	51.3	
4	0	3152	2920	48.1	4	0	2899	3057	51.3	
	L	1954	2112	51.9		L	2696	2898	51.8	
	M+H	828	594	41.8		M+H	1462	1193	44.9	
5	0	1322	4693	78.0	5	0	911	3681	80.2	
	L	723	2475	77.4		L	663	2231	77.1	
	M+H	1103	2823	71.9		M+H	1244	2506	66.8	
6	0	1548	5721	78.7	6	0	1131	4480	79.8	
	L	972	3306	77.3		L	825	2725	76.8	
	M+H	1416	3194	69.3		M+H	1497	3174	68.0	
		<i>s.e.m. (%)</i>	<i>normalized(%)</i>	avg (EdU+%)			<i>s.e.m. (%)</i>	<i>normalized(%)</i>	avg (EdU+%)	
	0	7.4	90.3	71.0		0	7.0	89.2	70.1	
	L	6.1	89.3	68.9		L	6.0	87.5	67.5	
	M+H	6.7	81.9	58.3		M+H	5.9	77.7	55.2	

Supplemental References

Corish, P., and Tyler-Smith, C. (1999). Attenuation of green fluorescent protein half-life in mammalian cells. *Protein Eng* 12, 1035-1040.

Schönthal, A. H. (2004). Checkpoint controls and cancer, (Totowa, N.J.: Humana Press).

Shaner, N. C., Campbell, R. E., Steinbach, P. A., Giepmans, B. N., Palmer, A. E., and Tsien, R. Y. (2004). Improved monomeric red, orange and yellow fluorescent proteins derived from *Discosoma* sp. red fluorescent protein. *Nat Biotechnol* 22, 1567-1572.